inverted in Fig. 2*c*) and the novel scheme (Fig. 2*d*). Note that the eye diagram shown in Fig. 2*d* is logically inverted compared to the back-to-back signal due to the reasons explained above. Furthermore, the synchronisation between the data and clock signal is achieved manually in these experiments (using an optical time delay). It is emphasised that all results are obtained using the same Mach-Zehnder interferometer and that the device has been optimised for each specific experiment. As seen, superior speed performance is clearly achieved with the proposed scheme, where there is a clear separation between the eyes.

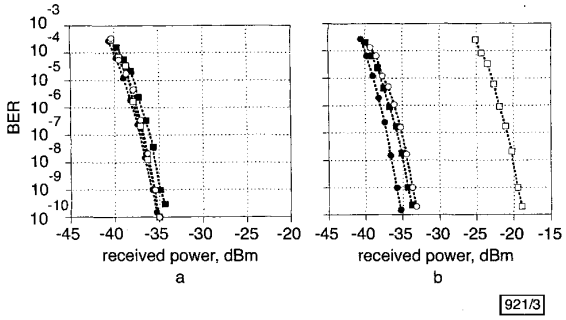


**Fig. 3** *BER measurements at 10Gbit/s for back-to-back signal and converted signal using conventional and proposed schemes*

*a* Before transmission
*b* After transmission over 25km standard fibre
● back-to-back
■ non-inverting (converted)
□ inverting (converted)
○ inverting (proposed)

To assess the transmission properties of the converted signals, the two methods were compared. The results can be seen in Fig. 3, giving the BER as a function of the received power for the back-to-back signal and the converted signals using the conventional and novel scheme. Fig. 3*a* shows the BER before transmission, while Fig. 3*b* shows the BER after transmission over 25km standard fibre. As seen in Fig. 3*a*, nearly penalty-free conversion is performed with the two schemes. The highest penalty is observed for conventional non-inverting operation, which primarily is due to the lower modulation bandwidth (see also Fig. 2); however, as seen in Fig. 3*b*, there is a difference after transmission. Inverting operation using the conventional scheme results in a pre-amplified penalty of ~17dB due to the chirped output signal, whereas non-inverting operation using the conventional scheme and conversion using the novel scheme results in an almost equal pre-amplified penalty of only ~2dB. These results verify the very important advantage of the novel conversion scheme, namely excellent transmission properties while at the same time exhibiting a superior modulation bandwidth. As seen by comparing Figs. 2 and 3, this is clearly not the case for the conventional scheme.

*Conclusion:* A novel scheme for all-optical wavelength conversion in SOA-based interferometric devices has been investigated experimentally and compared to the conventional conversion scheme. It has been demonstrated that, in contrast to the conventional scheme, the novel scheme results in excellent transmission properties while at the same time exhibiting the highest modulation bandwidth.


*29 June 2000*
*Electronics Letters Online No: 20001245*
*DOI: 10.1049/el:20001245*

D. Wolfson, T. Fjelde and A. Kloch (*Research Center COM, Technical University of Denmark, Bldg. 349, DK-2800 Lyngby, Denmark*)

E-mail: dw@com.dtu.dk

B. Dagens, C. Janz, F. Poingt, I. Guillemot, F. Gaborit, A. Coquelin and M. Renaud (*OPTO+, Groupement d'Intérêt Economique, Alcatel Corporate Research Center, Route de Nozay, 91460 Marcoussis, France*)

## References

1 MIKKELSEN, B., JEPSEN, K.S., VAA, M., POULSEN, H.N., STUBKJAER, K.E., HESS, R., DUELK, M., VOGT, W., GAMPER, E., GINI, E., BESSE, P.A., MELCHIOR, H., BOUCHOULE, S., and DEVAUX, F.: 'All-optical wavelength converter scheme for high speed RZ signal formats', *Electron. Lett.*, 1997, **33**, (25), pp. 2137–2139

2 WOLFSON, D., HANSEN, P.B., FJELDE, T., KLOCH, A., JANZ, C., COQUELIN, A., GUILLEMOT, I., GABORIT, F., POINGT, F., and RENAUD, M.: '40Gbit/s all-optical wavelength conversion in an SOA-based all-active Mach-Zehnder interferometer'. Proc. ECOC'99, Nice, France, 1999, Paper WeB4.5

3 WOLFSON, D., KLOCH, A., FJELDE, T., JANZ, C., DAGENS, B., and RENAUD, M.: '40Gbit/s all-optical wavelength conversion, regeneration and demultiplexing in an SOA-based all-active Mach-Zehnder interferometer', *IEEE Photonics Technol. Lett.*, 2000, **12**, (3), pp. 332–334

# Bit error rate performance of ultrashort-pulse optical CDMA detection under multi-access interference

S. Shen, A.M. Weiner, G.D. Sucha and M.L. Stock

The first system measurement on the bit error rate performance of an ultrashort-pulse optical CDMA channel under multi-access interference is reported. Effective interference suppression for error-free CDMA detection is demonstrated through spectral phase coding and the use of a nonlinear fibre discriminator.

*Introduction:* In an ultrashort-pulse code-division multiple-access (CDMA) fibre optic communications system, users share the same transmission media through spectral phase encoding and decoding of ultrashort optical pulses. The success of system operation depends on the effective suppression of multi-access interference [1]. Previously, an ultrashort-pulse CDMA test bed has been demonstrated [2], which includes the encoding of femtosecond pulses using a fibre-pigtailed grating/lens based pulse-shaper, dispersion compensation for distortionless fibre propagation of coded pulses, high-fidelity decoding, and subsequent nonlinear optical discrimination to distinguish correctly decoded data from incorrectly decoded multi-access interference at the receiver. Recent advances in compact photonic devices for spectral coding [3, 4] and in optical nonlinear discriminators [5] point to the technical feasibility of optical CDMA for local and metropolitan applications. However, all previous experimental studies of ultrashort-pulse CDMA were limited to a system with only one transmitter and one receiver. It is critically important to evaluate the effectiveness of CDMA interference suppression in a multiple-user environment. In this Letter, we report the first experimental study to our knowledge on multi-access interference suppression in an ultrashort-pulse CDMA system. Our measurements on the performance of a signal channel in the presence of crosstalk from an interfering CDMA channel demonstrate almost total interference suppression, resulting in a measured bit error rate below $10^{-11}$.

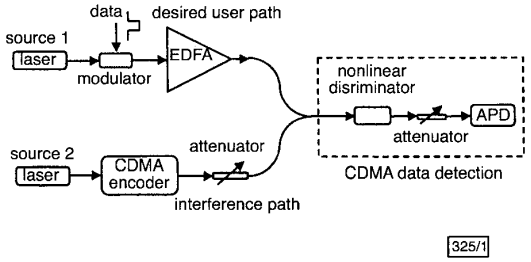


**Fig. 1** *Experimental setup of CDMA system BER measurements*

*Experiments and results:* The suppression of interference in an ultrashort-pulse CDMA system is achieved primarily through pseudorandom spectral phase coding and the use of a nonlinear optical discriminator. At each CDMA receiver, correctly decoded data from the desired user are restored to clean ultrashort pulses

with relatively high-peak intensity, while incorrectly decoded multi-access interference appears as a pseudonoise-like signal. A discriminator detects the peak power of the correctly decoded signals and suppresses the low intensity noise based on nonlinear optics. To evaluate the efficacy of multi-access interference suppression, we performed back-to-back measurements in an ultrashort-pulse CDMA system with two users - one as a desired user and the other as an interfering user. Fig. 1 shows the schematic diagram of our experimental setup. At the transmitter side, we used a home-built passively modelocked fibre laser (source 1 in Fig. 1) to provide a 40MHz train of ultrashort pulses for the desired user. The nearly transform-limited laser output (FWHM pulsewidth ~480fs) was synchronously modulated at 40Mbit/s with a length $2^{23}$–1 pseudorandom bit stream (PRBS) data. We used another modelocked Er:fibre laser (a Femtolite B-35 from IMRA, Inc) as the broadband source for the interfering user (source 2 in Fig. 1). It generates transformed-limited pulses of ~430fs (FWHM pulsewidth) repeated at 50MHz The interfering user's pulse train was not modulated in these experiments. The spectra of both lasers were centered at 1560nm.

Laser pulses from the interfering user (source 2) were launched into a fibre-pigtailed femtosecond pulse-shaper equipped with a 128-pixel liquid-crystal phase modulator (LCM) array [2] for spectral phase coding. Pseudorandom *M*-sequence phase codes with various code lengths were applied in the LCM in experiments. After being combined with modulated data from the desired user through a 1×2 fibre coupler, the coded pulses emulate the incorrectly decoded multi-access interference in a complete lightwave CDMA system. At the receiver side, we used a nonlinear discriminator based on self-phase modulation (SPM) in an optical fibre to suppress the incorrectly decoded noise for error-free CDMA data detection. An avalanche photodetector (APD) with a bandwidth of ~550MHz was used after the discriminator. For simplicity, we omitted spectral phase coding both after source 1 and in the CDMA receiver. Hence the uncoded pulses from source 1 emulate correctly decoded CDMA signals from a desired user. The fibre discriminator used here consists of a dispersion-shifted fibre (DSF, zero-dispersion wavelength is 1560nm) followed by a long-wavelength pass filter with 1572nm cut-off, which transmits very little of the input light unless there are frequency shifts arising from SPM in the fibre. The design and its operation have been reported in the references [2, 6]. Both the signal and interference paths before the discriminator were dispersion compensated using dispersion-compensating fibres.

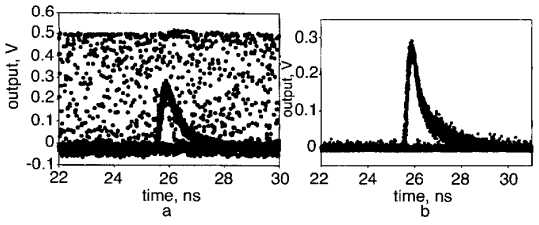


**Fig. 2** *Eye-diagrams of CDMA signals under multi-access interference*

*a* Without phase coding in the interference path
*b* With length-63 *M*-sequence phase coding in the interference path

In the experiments, the average power of CDMA data (source 1) was fixed at 250μW before the discriminator, which yields sufficient nonlinearity in the DSF to generate as much as 10μW output power after the long-wavelength pass filter. For error rate measurements, the received signal power at the APD was varied from –44 to –37dBm. To evaluate CDMA detection under large interference conditions, we always kept the interference power before the APD at –30dBm when no phase coding was added in the interference path. This was achieved by adjusting the input interference power before the discriminator. Note that if no phase coding is used, the interference level is at a minimum 7dB higher than the signal level at the APD. To show interference suppression, we first compared the eye-diagrams of the signal channel (set at –44dBm before the APD) with and without a length-63 *M*-sequence phase code applied to the interference path. The eye-diagram in Fig. 2*a* shows that, without phase coding, the desired data are completely buried under the multi-access interference. Note that the interference power here is 14dB larger than the signal power and has already saturated the APD receiver. The eye-diagram in Fig. 2*b* demonstrates that coding together with the fibre discriminator strongly suppress this large interference, resulting in a clean and open eye. Fig. 3 shows the BER performance of the signal channel when the length of the *M*-sequence phase coding in the interference path was varied. For *M*-sequence code lengths of 7, 15, 31, and 63, the interference power was suppressed to 10nW, 1.7nW, 0.6nW and 0.1nW (40dB suppression!), respectively. For comparison, the BER of the signal channel without interference is also shown in Fig. 3. We note that as the coding length in the interference path increases the power penalty to CDMA signal detection decreases substantially. When the code length reaches 63, the power penalty caused by the interfering user is almost zero. The decreased power penalty implies that with larger spectral phase coding length, more users could be supported simultaneously in a system. Since in our experiment the interference power before the APD when no phase coding is used is purposefully set to be much larger than the signal power, our results provide evidence for the possibility of error-free CDMA detection with a large number of users in the system.

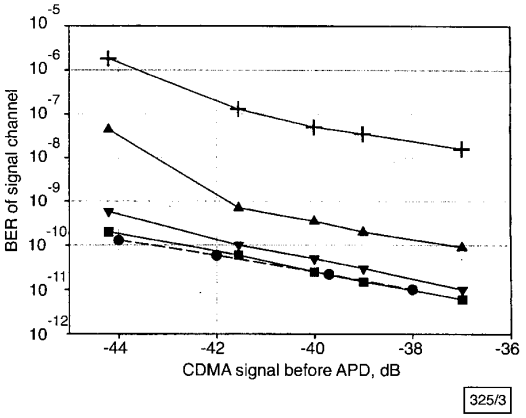


**Fig. 3** *BER of ultrashort-pulse CDMA channel without interference and under interference with the M-sequence code length of 63, 31, 15, and 7*

● without interference
■ code length of 63
▼ code length of 31
▲ code length of 15
\+ code length of 7

*Conclusion:* We have reported the first bit error rate measurement of an ultrashort-pulse optical CDMA channel under multi-access interference. Our results show that the suppression of interference in a CDMA system depends critically on spectral phase coding length and nonlinear optical discrimination.


*24 July 2000*
*Electronics Letters Online No: 20001259*
*DOI: 10.1049/el:20001259*

S. Shen and A.M. Weiner (*School of Electrical & Computer Engineering, 1285 EE Building, Purdue University, West Lafayette, IN 47907, USA*)

E-mail: shuai@ecn.purdue.edu

G.D. Sucha and M.L. Stock (*IMRA America, Inc., 1044 Woodridge Ave., Ann Arbor, MI 48105, USA*)

## References

1 SALEHI, J.A., WEINER, A.M., and HERITAGE, J.P.: 'Coherent ultrashort light pulse code-division multiple access communication systems', *J. Lightwave Technol.*, 1990, **8**, (3), pp. 478–491

2 SARDESAI, H.P., CHANG, C.C., and WEINER, A.M.: 'A femtosecond code-division multiple-access communication system test bed', *J. Lightwave Technol.*, 1998, **16**, (11), pp. 1953–1964

3 TSUDA, H., TAKENOUCHI, H., ISHII, T., OKAMOTO, K., GOH, T., SATO, K., HIRANO, A., KUROKAWA, T., and AMANO, C.: 'Spectral encoding and decoding of 10Gbit/s femtosecond pulses using high resolution arrayed-waveguide grating', *Electron. Lett.*, 1999, **35**, (14), pp. 1186–1188

4 GRUNNET-JEPSEN, A., JOHNSON, A.E., MANILOFF, E.S., MOSSBERG, T.W., MUNROE, M.J., and SWEETSER, J.N.: 'Fibre Bragg grating based spectral encoder/decoder for lightwave CDMA', *Electron. Lett.*, 1999, **35**, (13), pp. 1096–1097
5 ZHENG, Z., SHEN, S., SARDESAI, H.P., CHANG, C.C., MARSH, J.H., KARKHANEHCHI, M.M., and WEINER, A.M.: 'Ultrafast two-photon absorption optical thresholding of spectrally coded pulses', *Opt. Comm.*, 1999, **167**, (1-6), pp. 225–233
6 SARDESAI, H.P., and WEINER, A.M.: 'Nonlinear fibre-optic receiver for ultrashort pulse code division multiple access communications', *Electron. Lett.*, 1997, **33**, (7), pp. 610–611

## Optical BPSK subcarrier modulation using integrated hybrid device

M. Shin, J. Lim, J. Kim, C.Y. Park, J.S. Kim, K.E. Pyun and S. Hong

An integrated optical/RF hybrid device has been designed and fabricated for binary-phase-shift-keying subcarrier modulation. The device has been used to directly modulate an RF subcarrier of 10GHz in a BPSK scheme with an independently applied RF carrier and digital signal.

*Introduction:* Microwave- and millimetre-wave (MMW) RF resources are receiving increasing attention since they are capable of providing wide-band channels required for both mobile communication systems and wireless local area networks [1]. To realise such systems, an approach involving optical and RF hybridisation is proposed. Hybrid fibre/coax networks enable robust transmission of an RF subcarrier signal via a singlemode fibre, thus enabling a significant reduction in the number of cascade RF amplifiers to be achieved. Microwave- and millimetre-wave digital transmission systems using QPSK or BPSK modulation have been reported [2].

Although MMW bands have a capacity of > 1Gbit/s, previous works have reported data transmission of only several hundred Mbit/s [3]. This is due to the lack of a proper modulation scheme for the hybrid approach. In general, up-conversion schemes in the transmitter use an intermediate frequency to convert the base band-signal to the MMW band, with the result that the data rate cannot exceed the intermediate frequency. There is also a need for high frequency amplifiers and mixers, which are very difficult to implement if the MMW carriers are to be used at full capacity.

We propose a binary phase shift method using a single integrated hybrid device. The device is composed of two identical high-speed multiple quantum well (MQW) electroabsorption (EA) modulators branched with two multimode interference (MMI) couplers. The phase of the RF carrier changes as a result of optical amplitude modulation of the modulators and of the interference resulting from the phase delay at the MMI couplers. The results of the modulation operation of the device in the low frequency region have been presented [4]. In this Letter, BPSK modulation of a 10GHz signal is reported. The $f_{3dB}$ bandwidth of the device and the frequency spectrum of the modulated optical signal are also measured.

*Device fabrication:* The device structure is illustrated in Fig. 1. The input 3dB MMI coupler divides and branches incident light into two identical MQW EA modulators. The MMI couplers are designed to have a paired interference mirror image with the same amplitude but $\pi/2$ phase difference [5]. Since the two identical MMI couplers are placed at both the input and output ports as shown in Fig. 1, the output of the device produces an out-of-phase image, which causes the optical fields to interfere destructively. On the other hand, the amplitude of the signal in each branch is varied when it passes through the EA modulator. A digital on-and-off signal (0 or 1) is applied to the modulator $M_1$ to switch the operation state, and an RF carrier signal is applied to the modulator $M_2$. When a reverse voltage is applied to modulator $M_1$ (OFF state), the out-of-phase output decreases as the reverse voltage to $M_2$ is increased. In contrast, when $M_1$ is biased with 0V (ON state), the output increases with the reverse voltage at $M_2$. This is due to the fact that, when $M_1$ is on, the difference between the optical outputs from the two modulators increases at the output port as $M_2$ becomes opaque. Thus, the phase of the RF carrier generated at modulator $M_2$ is shifted by $\pi$ depending on the state of modulator $M_1$. Since the subcarrier and the digital data are introduced independently to the modulators, the subcarrier frequency and the data rate are limited only by the bandwidth of the high-speed EA modulators. Therefore, the direct up-conversion from the base-band to the MMW band can be achieved when modulators with a 3dB bandwidth of several ten gigahertz are provided. In addition, synchronisation of a local oscillator to generate RF subcarrier and digital signal is not necessary in this scheme. This is because with this modulation mechanism the signal phase changes at an arbitrary time instant as a result of optical interference.

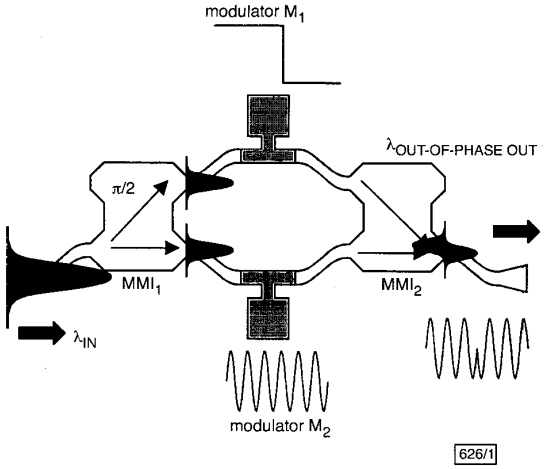


**Fig. 1** *Integrated optical/RF hybrid device*
Input optical signal undergoes phase change of $\pi$ when it passes through two mirror image MMIs

The device was fabricated in the following process. The epitaxial layers of the modulator region were prepared on an $n^+$-InP substrate by metal organic chemical vapour deposition (MOCVD). Multiple quantum well (MQW) absorption layers of 250nm thickness were grown between graded-index clads of 70nm thickness. The MQW layers consisted of ten pairs of 1.52 Q-InGaAsP wells ($\lambda_g$ = 1.52μm) of 10nm thickness and 1.2 Q-InGaAsP barriers ($\lambda_g$ = 1.2μm) of 6.5nm thickness. The low-loss passive region was grown by butt-coupled regrowth. Deep dry etching was applied to form the waveguide structures including MMI couplers and MQW EA modulators. A 3μm thick polyimide was employed to block the leakage current and to reduce the pad capacitance [4].

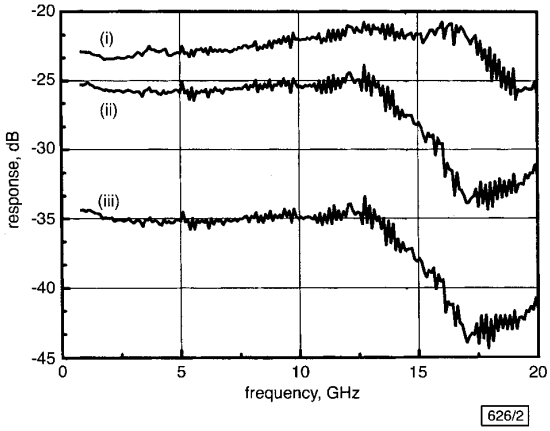


**Fig. 2** *Small signal frequency response of MQW EA modulator at bias voltage of −1 V for optical wavelength λ and length of modulator L*
(i) λ = 1530nm, $L$ = 100μm
(ii) λ = 1530nm, $L$ = 150μm
(iii) λ = 1550nm, $L$ = 150μm

*Measurement results:* The characteristics of the MMI couplers and EA modulators strongly depend on the wavelength and polarisa-